Effect of Surface Treatment on the Physicomechanical and Thermal Properties of High-Density Polyethylene/Olive Husk Flour Composites

C. Ihamouchen,[1] H. Djidjelli,[1] A. Boukerrou,[1] S. Krim,[1] M. Kaci,[1] J. J. Martinez[2]

[1]*Organic Materials Laboratory, Department of Genie of Processes, University A. Mira, Targa-Ouzemmour, Bejaia 06000, Algeria*
[2]*Genie Electric Laboratory (UMR-CNRS 5003), University Paul Sabatier, Toulouse 31400, France*

Received 17 November 2009; accepted 16 January 2011
DOI 10.1002/app.34172
Published online 15 August 2011 in Wiley Online Library (wileyonlinelibrary.com).

ABSTRACT: In this study, a particular interest was focused on the recovery of lignocellulosic waste of olive husk flour (OHF) by its incorporation as filler in manufacturing composite materials based on high-density polyethylene (HDPE) matrix with various filler contents (10, 20, and 30 wt %). The problem of incompatibility between the hydrophilic filler and the hydrophobic matrix was treated with two methods: the first method consists of using maleic anhydride-grafted polyethylene (MAPE) as compatibilizer in HDPE/OHF composites. The second method, was focused on the chemical modification of OHF by vinyl-triacetoxy-silane (VTAS). Fourier transform infrared spectroscopy is used to analyze both grafting and silanization reactions involved. Scanning electron microscopy was used to show the morphology of the flour surface. Furthermore, the physicomechanical and thermal characteristics of the various composite samples were investigated as a function of filler contents and treatment types. The results showed that the properties of the composite materials are positively affected by the silanization treatment of OHF and also by MAPE addition. However, better mechanical and thermal properties with less moisture absorption were obtained for the composite materials compatibilized with MAPE. © 2011 Wiley Periodicals, Inc. J Appl Polym Sci 123: 1310–1319, 2012

Key words: composites; fibers; polyethylene; compatibilization; modification

INTRODUCTION

Natural fiber-reinforcing composites have attracted the attention of scientists and industrialists community because they are turning out to be an alternative solution to the ever-depleting petroleum sources. As a result of the increasing demand for environmentally friendly materials, many natural fiber composites have been developed and tend to integrate an ecological character.[1] Natural fibers like banana, cotton, sisal, jute, and olive husk flour (OHF) exhibit a number of attractive features, including low density, abundance, and certainly biodegradability, and efficient production technologies, including extrusion and injection molding.[2,3] These composites are being used in a large number of applications, including automotive, interiors, building industry, and many other furniture.[4]

Commodity thermoplastics are mostly used in the manufacture of plastic/wood filler composites. Among these thermoplastics, high-density polyethylene (HDPE) is one of the most important thermoplastics because of its good properties, i.e., fluidity, flexibility, and electrical insulation.[5] The olive husk, one of the several lignocellulosic materials, is an agricultural industrial residue produced as by-products during the olive milling process in the olive-producing countries such as Algeria. Every year, thousands of tons of this product are incinerated or rejected in the wild, causing major inconvenience to the environment.

Despite the advantages, the use of natural fiber has been restricted because of its inherent high moisture absorption capacity, thermal instability during processing, poor wettability, and poor adhesion toward polyolefins.[6,7] The surface characteristics of the natural fibers, such as wetting, adhesion, surface tension, or porosity of fibers, can be improved through chemical modification. In the literature, several strategies have been suggested describing the way to improve the compatibly of lignocellulosic fibers with thermoplastic polymers,[8] such as esterification, silane treatment, graft copolymerization, use of compatibilizers, plasma treatment, and treatment with other chemicals. The chemical treatment of wood filler or the functionalization of the polymer usually requires the use of reagents, which contain functional groups

Correspondence to: C. Ihamouchen (ihchadou@yafoo.fr).

that are capable of reacting and forming chemical bonds with the hydroxyl groups of the lignocellulosic material. The literature has reported more than 40 coupling agents used in composite wood fiber/synthetic polymer.[9] A lot of research was devoted to composites based on HDPE and lignocellulosic fillers[10,11]; however, only few works were published on polymer composites loaded with OHF. In this study, a particular interest was focused on the recovery of lignocellulosic waste of OHF by its incorporation as filler in manufacturing composite materials based on HDPE matrix. Composites based on HDPE and treated OHF with vinyl-triacetoxy-silane (VTAS) was studied. The results obtained were compared with those of HDPE and untreated OHF (UTOHF) composites compatibilized with maleic anhydride grafted polyethylene (MAPE) synthesized in the laboratory. Moreover, the effects of the various treatments on the chemical structure and physical properties of the composites were also investigated.

EXPERIMENTAL

Materials

HDPE was provided by the National Company "ENIP" (Bejaia, Algeria) under the grade name POLYMED 6030. The polymer has the density of 0.960 g/cm^3 and a melt flow index of 2–3 g/10 min. The VTAS was produced by Sigma Aldrich Company (Germany). The main characteristics of the product are as follows: density = 1.167; melting point = 76°C; and boiling point = 126–128°C.

MAPE was synthesized in the laboratory and used as a coupling agent. The main characteristics of the product are as follows: the quantity of MA grafted onto the HDPE molecules was determined by titration of acid groups derived from the anhydride function, it was estimated at 1.55%. The mechanical properties are as follows: $E = 542$ MPa; $\sigma = 34$ MPa; and $\varepsilon = 28\%$.

The olive husk (OHF) of a granular form was obtained from the olive treatment plant in the region of Bejaia in Kabylia (Algeria). Prior to any chemical modification and mixing with the HDPE, the olive husk was first air dried for 2 weeks and ground into very thin particles. The size fraction selected after sifting the olive husk has a maximum average diameter of 90 μm. This is more suitable for a homogeneous dispersion in the thermoplastic matrix. The major constituents of the OHF were determined on the basis of absolutely dry substances using chemical procedures[10] (i.e., cellulose = 39 ± 0.5 wt %; lignin = 20.52 ± 0.4 wt %; organic content = 8.5 ± 0.8 wt %; and mineral filler = 3 ± 0.2 wt %; the moisture content of the filler was 7 ± 0.3 wt %).

Grafting procedure

The grafted HDPE was synthesized in a solution state. According to the procedure reported previously by Garcia Martinez et al.,[12] the mixture contains 10 g of polyethylene, 2.5 g of anhydride maleic, and 100 mL of xylene. The mixture was then stirred under inert atmosphere (N_2) at 140°C up to complete dissolution. After adding 0.1 g of benzoyl peroxide to the mixture, the reaction took place for 3 h.

The grafted products were separated from the rest by precipitation and dissolved in 100 mL of refluxing xylene during 1 h, then filtered, and washed in acetone three times before drying under vacuum at 80°C for 12 h.

Flour characterization

The composition of lignocellulosic flours was determined according to the Acid Detergent Fiber-Neutral Detergent Fiber method.[13,14] The equilibrium moisture content was calculated by placing treated and untreated flours in a dessicator at 20°C and then drying them in an oven at 105°C until constant weight was reached. Three measurements were conducted for each sample, and the results were averaged to obtain a mean value.

Flour treatment

According to the procedure reported previously by Gassan and Bledzki,[15] 10 g of OHF were added into a mixture of methanol/water (90/10, w/w) and stirred for 12 h at room temperature. Then the flour was filtered and dried in an oven at 80°C for 12 h. For the flour surface treatment, 5 wt % of silane/weight of OHF were dissolved in a methanol/water mixture at room temperature, and the pH of the solution was adjusted to 4 with the addition of acetic acid. Silanes are more stable if they are applied from a slightly acid solution. After 10 min of stirring, the dried OHF were immersed in the solution and stirred for 24 h at room temperature. The OHF were then filtered and dried at 80°C for 12 h.

Preparation of composites

Various formulations based on HDPE, UTOHF, MAPE, and OHF treated with vinyl-triacetoxy-silane (OHFTS) were prepared, whose codes (UT: untreated; TS: treated with silane; TP: treated with MAPE) and compositions are reported in Table I.

Films were prepared by twin-roll milling process using a rotating speed of 28.5 rpm for the back cylinder and 29.8 rpm for the front one at 160°C and a residence time of 8 min. The gap between the rolls is roughly about 1 mm. Then the films were granulated and pressed into plates of 2 mm thickness by using a

TABLE I
Mass Composition of the Various PE Formulations

Components (wt %)	F0	F10 UT	F20 UT	F30 UT	F10 TS	F20 TS	F30 TS	F10 TP	F20 TP	F30 TP
HDPE	100	90	80	70	90	80	70	85	75	65
UTOHF	0	10	20	30	0	0	0	10	20	30
OUFTS	0	0	0	0	10	20	30	0	0	0
MAPE	0	0	0	0	0	0	0	5	5	5

hydrolic press Type "FONTJINE model TP400" Holland at 180°C and 250 kN during 5 min. The plates obtained were used for testing.

Spectroscopic analysis: Fourier transform infrared spectroscopy

The reaction product was qualitatively characterized by Fourier transform infrared spectroscopy (FTIR) using KBr pellet technique. Spectra were recorded using FTIR model Shimadzu FTIR-8400, with a resolution of 4 cm^{-1} within the region 4000 to 400 cm^{-1}.

X-ray diffraction

Measurements of X-ray diffraction (XRD) were performed using Cu-K line wavelength $\lambda = 1.54059$ Å. The source of X-ray tube is a ceramic with a copper anode and fed by a current of 45 kV and an intensity of 30 mA. Each scan was performed with a measurement time of 6.05 seconds per step. The range of angles swept is between 1° and 70°.

Tensile test

The tensile test is carried out by using a tensile machine of the type BTC-FR 2,5 TN.D09, according to the standard ISO 527, June 1993. The speed of deformation is maintained constant with 250 mm/min, and the curves strength–deformation are plotted, each value obtained represented the average of six samples.

Test of shore hardness D

The test consists in applying an effort tending to insert the needle of a shore D durometer following standard NF ISO T 51-123 to plates of 5×5 cm^2. The reading is done directly on the durometer after the penetration of 15 s.

Thermogravimetry analysis

Thermogravimetry analysis (TGA/DTG) is used to assess the loss of mass undergone by a sample during a heat treatment as a function of temperature. The apparatus used is SETAREM TGA 92, consisting of a TGA/DTG coupled and driven by a microcomputer. The experiments were conducted on samples of mass from 10 to 20 mg, which are built in a crucible and heated in platin in an inert nitrogen with a heating rate of 10°C/min and in a temperature range from 20 to 700°C.

Test of water absorption

Composite samples were used for measuring water absorption according to the following procedure: after being oven dried at 70°C for 24 h, the specimens were kept in the desiccators at room temperature. Then, the specimens were weighted before immersion in distilled water, and the corresponding mass was recorded as M_0. The specimens were periodically removed from the water bath, and the surface was dried with absorbent paper and weighed again. The corresponding mass was defined as M. Three specimens were tested for each compound and the average readings were recorded. Water absorption was calculated according to standard NF 51-002.

Scanning electron microscopy

Scanning electron microscopy (SEM) was performed with a FEI CONTA 200 microscope. Before the fracture, the specimens were frozen into liquid nitrogen to impede the plastic deformation of the matrix and to get well-defined fiber–matrix interface. The objective was to get some information regarding the filler dispersion and bonding quality between filler and matrix and to detect the presence of microdefects.

RESULTS AND DISCUSSION

Characterization of OHF

The various chemical components present in OHF are shown in Table II and are compared with different fibers. As shown in Table II, wood and paper flour contain high amounts of cellulose,[2] contrary to the OHF, which are rich in lignin material.

Fourier transform infrared spectroscopy

Untreated and silanized OHF were characterized by FTIR spectroscopy to confirm the chemical reaction between the silane and the OHF cellulose. Figure 1 shows the FTIR spectra of untreated and silanized

TABLE II
Chemical Composition of Lignocellulosic Flours

Chemical constituents (wt %)	Olive husk flour	Wood fibers	Paper flour
Cellulose	40.56	48	79.50
Lignine	23.43	24	3.50
Hemicellulose	18.10	15	8.30
Humidity	7.90	6.60	6.30
Others	14.00	13	8.50

OHF in the region 4000–400 cm^{-1}. Both of them reveals a large absorption band located in the range 3700 and 3050 cm^{-1}, which corresponds to the elongation vibrations of hydroxyl groups (—OH). After treatment, a slight decrease in the absorption band intensity of the hydroxyl groups is observed. According to the literature, these structural changes in the OHF after treatment suggest that the substitution reaction between hydroxyl groups of the OHF and silanols groups of VTAS may have occurred. This is in line with the results reported by Kaci et al.[16] and Bengtsson and Oksman.[17]

The silanization of OHF reveals an intense band around 570 cm^{-1} and 600 cm^{-1} and were assigned to the stretching of the Si—O—cellulose and —Si—O—Si— bonds, respectively. Such an absorption band for Si—O—cellulose assures that condensation reactions had occurred between the cellulose of the OHF and the silanol group, and the band for Si—O—Si is an indication of intermolecular condensation having occurred between adjacent silanol groups deposited on the flours. There is also one absorption band centered at 1040 cm^{-1} characteristic of Si—O—Si moieties, and this could be attributed to the substitution of OH groups from OHF by silanol groups (obtained during hydrolysis of silanes) using condensation reaction, indicating the occurrence of silanization reaction. The peak near 1095 cm^{-1} of the treated flour is related to the residual unhydrolyzed Si—O—CH_3 groups, and the weak intensity suggests that most of the silane adsorbed in these conditions was actually hydrolyzed.[18]

The reaction of silanization of OHF with silane modifying agent has been confirmed by FTIR spectroscopic analysis. In addition, the reaction mechanism proposed by Boufi et al.[19] is illustrated in Scheme 1. First, the acetoxyl groups in the silane are hydrolyzed to hydroxyl groups (silantriol). Second, the silanol groups created in the first step react either by condensation with hydroxyl groups of OHF by creating covalent bonds (OHF—O—Si) or they react with hydrogen bonding or condensation with adjacent silanols groups (Si—O—Si). Finally, the hydrophobic part of the silane on the flour surface could chemically bond or interact through Van der Waals forces with the PE matrix.

Thermogravimetric analysis

The TGA/DTG thermograms of untreated and treated OHF recorded in the temperature range of 20–700°C are presented in Figure 2. It is noticed that the onset decomposition temperature of the UTOHF is slightly higher then the OHFTS. This reduction in the initial temperature of decomposition can be attributed to the elimination of some hydrogen bonds that requires significant energy to break them. We clearly see that the thermal degradation profile of untreated and treated OHF is similar. We observed a slight mass loss around 100°C, which can be attributed to water evaporation.

A second peak corresponds to the thermal degradation of hemicellulose and cellulose, and it is located between 200 and 300°C. More specifically, the thermal decomposition of cellulose occurs mainly by depolymerization from 300°C.[20] Indeed, when subjected to very high temperatures, cellulose absorbs enough energy causing the rupture of the glucosidic link. The depolymerization can also be accompanied by dehydration of the sugar giving rise to unsaturated compounds and the formation of various volatile compounds. Hemicellulose is less thermally stable than cellulose, and it degrades between 200 and 260°C. Although they represent a smaller fraction in the filler, it can significantly affect the thermal behavior of the composite because of the association with other structural components. In a study of jute fiber and its components by Bhaduri et al.,[21] they attributed this process to pyrolysis of the hemicellulose fraction. The thermal decomposition of lignin begins starting from 200°C. This decomposition can be explained by the cleavage of carbon–carbon bond between the structural units of lignin and dehydration reactions.[22] The residue

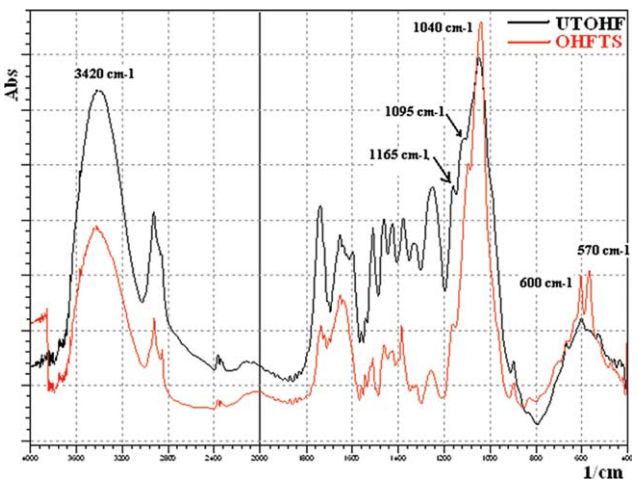

Figure 1 FTIR spectra of the olive husk flour treated and untreated. [Color figure can be viewed in the online issue, which is available at wileyonlinelibrary.com.]

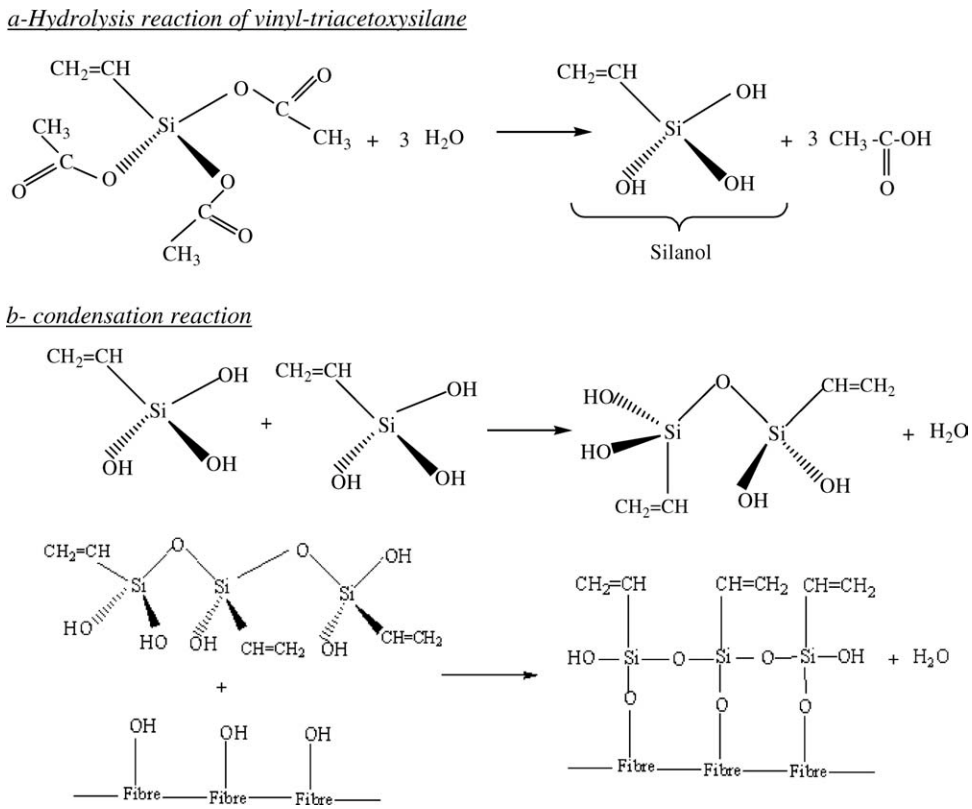

Scheme 1 Reaction of hydrolysis and condensation of silanes with a cellulosic fiber.

consisting mainly of ash is basically stable beyond 500°C. These results are in agreement with those of Ersan et al.[23]

X-ray diffraction

Figure 3 shows the XRD spectra of untreated and treated OHF. The spectrum of untreated OHF exhibits well-defined peaks at 2θ, i.e., 16.7° is probably due to one of the (110) or (1$\bar{1}$0) planes, 22 correspond to the (200) crystallographic plane, and 34.48° correspond to the (023) or (004) planes.[24] The spectrum of OHFTS shows the same peaks as that of UTOHF, but with higher intensity and the shift of peaks to 2θ larger values. This means that the inter-reticular distance "*d*" becomes smaller, i.e., the meshes become closer, thus explaining the destruction of hydrogen bonds. According to Panayiotou et al.,[2] when the cellulose content is higher in wood filler, there are two peaks near the 16° reflection; however, in our case, the high amount of amorphous materials such as lignin and hemicelluloses showed a single peak.

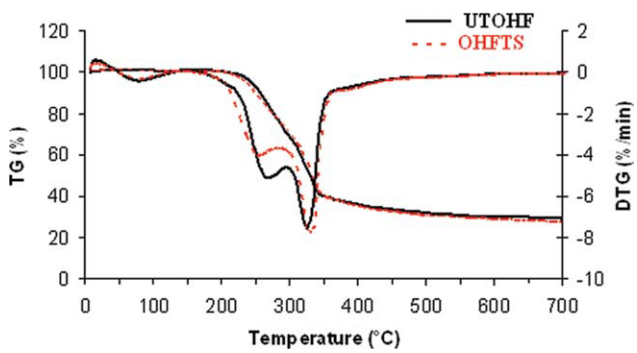

Figure 2 The TGA/DTG thermogram of olive husk flour treated and untreated. [Color figure can be viewed in the online issue, which is available at wileyonlinelibrary.com.]

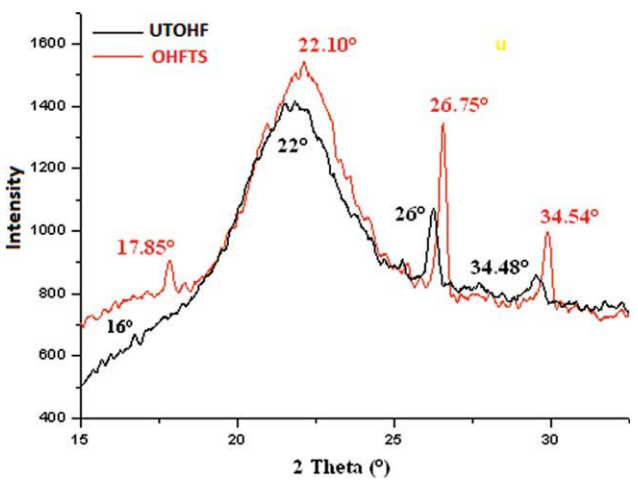

Figure 3 XRD spectra of the untreated olive husk flour and treated with vinyl-triacetoxy-silane. [Color figure can be viewed in the online issue, which is available at wileyonlinelibrary.com.]

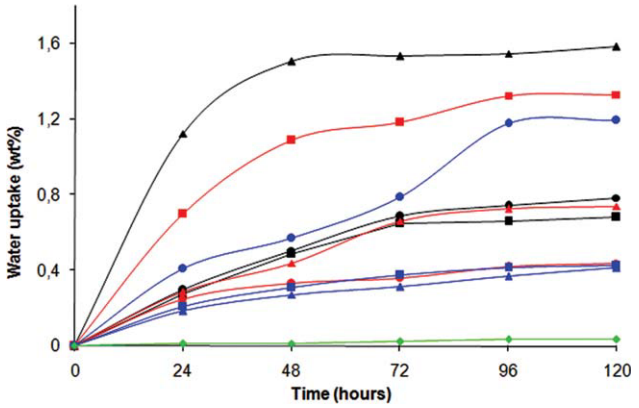

Figure 4 Evolution of the rate of water absorption of PE/OH composites (green-colored diamond, HDPE virgin), untreated (black square, UT10; black circle, UT20; and black triangle, UT30), silane treated (red-colored circle, TS10; red-colored triangle, TS20; and red-colored square, TS30), and MAPE treated (blue-colored triangle, TP10; blue-colored square, TP20; and blue-colored circle, TP30) as a function of time. [Color figure can be viewed in the online issue, which is available at wileyonlinelibrary.com.]

After treatment, the rate of crystallinity decreased from 45% corresponding to UTOHF to 34%. This decrease was attributed to the increase in the amorphous part. Shiraishi et al.[25] reported that esterification of cellulose with different chemical reagents takes place in the amorphous regions and proceeds by two different rates (rate of diffusion and rate of chemical reaction). The reagent first reacts with the chain ends on the surface of the crystallites, as it cannot diffuse into the crystalline region, resulting in the opening of some of the hydrogen-bonded cellulose chains. This procedure results in the formation of some new amorphous cellulose. Then, the reagent diffuses into this amorphous part, reacting with the cellulose and simultaneously generates more amorphous cellulose. These steps take place concurrently and depend on each other. Marcovich et al.[26] demonstrated that treatment of wood flour with maleic anhydride led to a decrease in crystallinity. Similar behavior was found by Bing et al.[27] for jute fiber and wood modified with different reagents.

Characterization of composites

Water absorption test

The evolution of water absorption of the HDPE/OHF composites versus time is shown in Figure 4. We can clearly see an increase in the absorption rate of water with immersion time for the UTOHF, which is quite expected. Boufi et al.[19] and Dufresne et al.[28] have found the same result and explained that the OHF is highly rich in hydroxyl groups and that they form hydrogen bonds with water molecules. For the virgin PE, there is very low water absorption due to apolar nature of this polymer and its hydrophobic character. After treatment, the rate of water absorption decreases. This result can be attributed to a diminution of the concentration of —OH groups of the cellulosic filler. However, the hydrophilic character is more pronounced for the composite treated with the modifying agent (VTAS) when compared with the compatibilized composites treated with MAPE.[16,19]

Mechanical properties of PE/GO composites

The evolution of the mechanical properties of untreated and treated PE composites as a function of flour loadings is presented in Table III. It has been observed that the tensile strength and elongation at break of the untreated HDPE/OHF composites decrease linearly with increasing the flour loading up to 30%. These results are expected and in agreement with the literature. Joong-Hyun et al.,[4] Kaci et al.,[16] and Djidjelli et al.[29] have attributed this decline to the decrease in bond strength between the filler and the matrix which obstructs the spread of effort. This decline increases when the flour loading becomes higher; this phenomenon can be explained by the tendency of particles of OHF to form agglomerates that induce heterogeneities and not uniform

TABLE III
Evolution of Mechanical Properties of Composites PE/OHF

Sample codes	Tensile strength (MPa)	Elongation (%)	Young's modulus (MPa)	Shore hardness D
F0	24.19 ± 0.58	14.1 ± 0.40	760.83 ± 49	60
F10 UT	23.65 ± 1.64	4.79 ± 0.81	794.9 ± 40	63
F20 UT	19.55 ± 1.37	4.65 ± 1.44	1071.81 ± 83	67
F30 UT	17.78 ± 1.06	3.76 ± 0.13	1162.6 ± 54	69
F10 TS	26.88 ± 0.70	4.73 ± 0.73	1469.8 ± 67	62
F20 TS	20.85 ± 1.50	3.76 ± 0.32	1417.83 ± 25	66
F30 TS	18.5 ± 0.39	3.43 ± 0.44	1364.39 ± 41	68
F10 TP	30.58 ± 0.89	6.86 ± 0.57	1179.33 ± 83	62
F20 TP	30.05 ± 0.74	5.92 ± 0.55	820.6 ± 36	64
F30 TP	27.05 ± 0.39	4.82 ± 0.61	439.39 ± 29	66

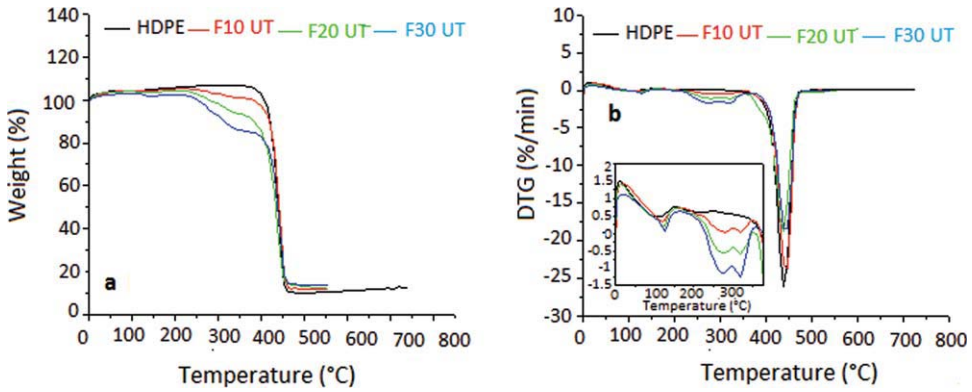

Figure 5 Thermal degradation behavior of the composites untreated: (a) TGA curves and (b) DTG curves. [Color figure can be viewed in the online issue, which is available at wileyonlinelibrary.com.]

strength within the matrix. The addition of UTOHF in the polyethylene matrix increases the rigidity of the composite, and this becomes stronger with the increasing of the flour content. This behavior can be explained by the rigid nature of OHF.

After chemical treatment, the stress at break increases. The high increase in the mechanical strength is primarily attributed to the reinforcing effect imparted by the flour, which allows a uniform stress distribution from continuous polymer matrix to dispersed flour phase and to improve interfacial adhesion resulting from some chemical bonding between the hydrophobic part of the silane–OHF surface and the PE matrix or van der Waals forces

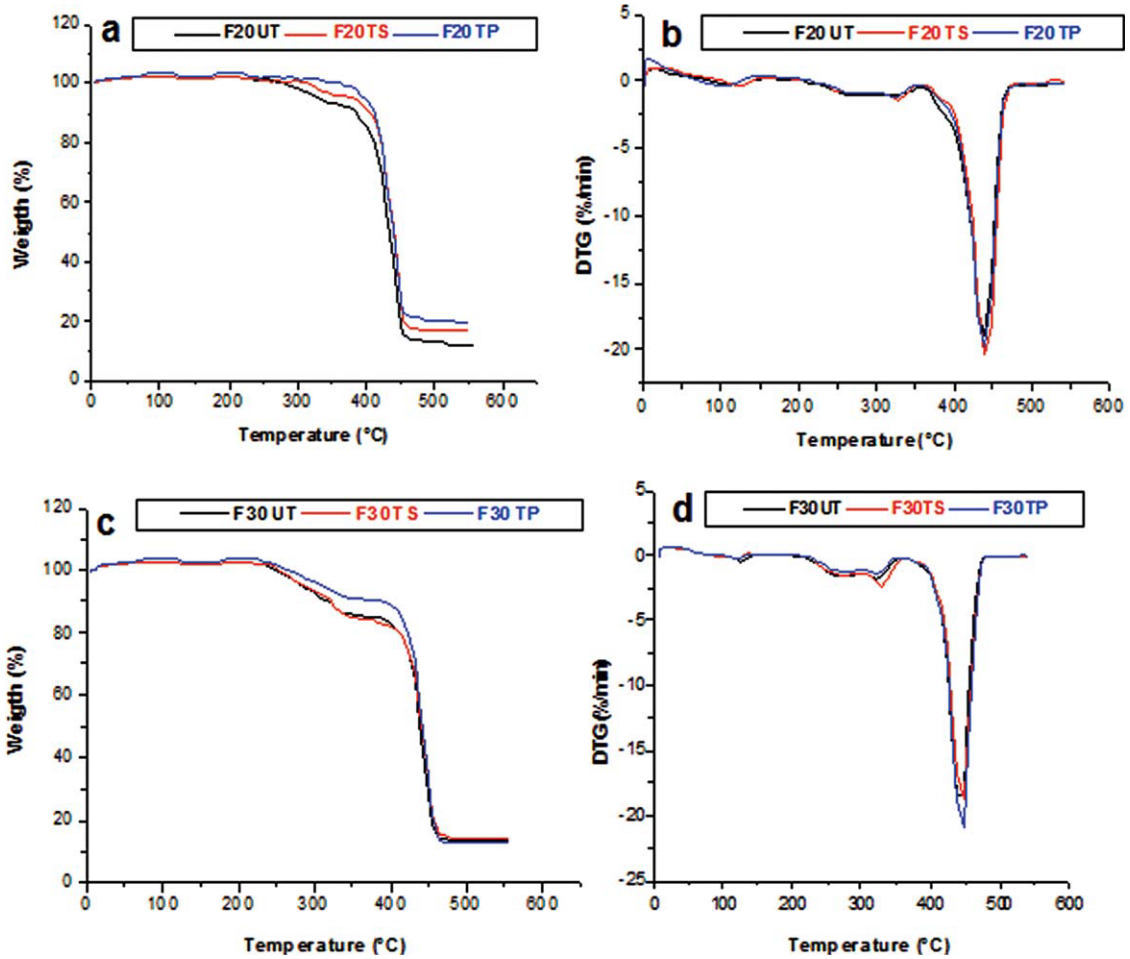

Figure 6 Thermal degradation behavior of the composites. TGA and DTG curves of the F20 formulation (a and b) and F30 formulation (c and d). [Color figure can be viewed in the online issue, which is available at wiley onlinelibrary.com.]

between them.[18] Moreover, covalent bonding is formed between the more accessible OH groups of OHF like hemicellulose and the anhydride moiety coming from the grafted PE. This result is confirmed by Sabu et al.[30] The addition of compatibilizer agent (MAPE) saves some of the elongation at break when compared with the untreated composites as indicated by the following results: 43.21, 27.31, and 28.19% corresponding to F10, F20, and F30 formulations, respectively, but not in terms of overall deformation when compared with virgin PE. This improvement is attributed to the good dispersion of the flour by adding the compatibilizer agent that gives flexibility to the material. We observed that the Young's modulus increases with the increase in UTOHF. This increase in the Young's modulus can be explained by the rigid nature of the OHF, and this is fundamentally linked to the formation of vacuum caused by the low interfacial adhesion between the matrix and UTOHF, which was confirmed by Dobircau et al.[31] For the F20 TP and F30 TP formulations, the Young's modulus decreases, which probably caused greater adhesion of interfacial OHF–PE composites when compared with untreated OHF, as explained by Demir et al.[32] Furthermore, we noticed that the addition of treated flour with vinyl-silane induces a little improvement in the deformation, but increases the Young's modulus.

The incorporation of the UTOHF increases the hardness. This increase is even greater when the rate of flour is high. This can be explained by the rigid character of OHF that increases the stiffness of the composite samples. After chemical modification, the hardness decreases. This is in agreement with the results reported by Sabu et al.,[30] and they have attributed this to the plastic coating of flour after treatment. This makes the composite samples less harsh, leading to nonbrittle behavior.

Thermal characterizations of PE/GO composites

Figure 5 shows the TGA-DTG thermograms of different composites prepared with untreated loadings. Therefore, the thermal behavior of the composite is the sum of the individual constituents of both the filler and the matrix. We noticed that the addition of the UTOHF in the PE matrix decreases the onset decomposition temperature, and this decrease becomes higher with the flour content. This decrease was confirmed by Ersan et al.[23] and was attributed to the presence of three main components (cellulose, hemicellulose, and lignin) in OHF. Around 460°C, there is a level of stability, which is attributed to the formation of a residue. The residual mass obtained at high temperature ($T = 600$°C) increases with increasing the flour content. For example, there are 11.72, 12.03, and 13.36% residue

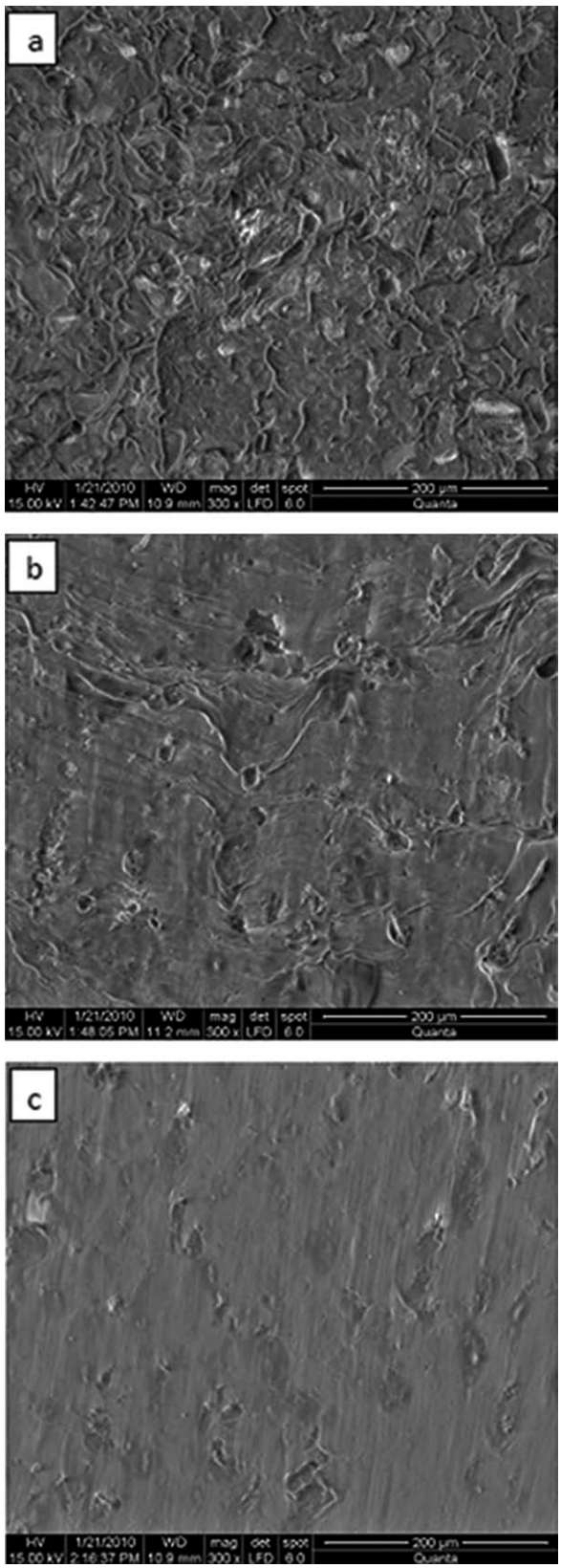

Figure 7 Scanning electron micrographs of fractured surface of OHF/HDPE composite loading at the 20 wt %: (a) composite untreated, (b) composite treated with silane, and (c) composite treated with MAPE; ×300.

in the samples of F10, F20, and F30 formulations, respectively.

The curves of TGA-DTG of the composites treated are shown in Figure 6. We clearly see that the profiles of thermal degradation of composites are similar. However, the composites modified by the MAPE reveal better thermal stability when compared with the composites modified by the VTAS and untreated composites.

Scanning electron microscopy

SEM micrographs of the fractured surface of HDPE-based composite reinforced with 20 wt % are shown in Figure 7. For the untreated composites [Fig. 7(a)], we can see the presence of many voids and cavities on the surface, indicating that the particles of OHF are pulled out from the matrix during fracture. This observation clearly indicates that the interfacial adhesion between the cellulosic filler and the polymer matrix is very weak. The presence of flour aggregates provides an evidence of poor dispersion of the filler within the polymeric matrix.[33]

On the other hand, the SEM micrographs of the modified fillers with silane and MAPE compatibilizer [Fig. 7(b,c), respectively] seem to provide better and finer dispersion of the cellulosic fillers in HDPE and probably show that a strong interfacial adhesion has occurred between the OHF and the polymer matrix. This behavior is due to the surface chemical modification, which confers a nonpolar character to the surface of the cellulosic fillers.[34] However, the addition of MAPE seems to enhance better the direct contact between the lignocellulosic fillers and the polymer matrix than the untreated and silane-treated composites.

CONCLUSION

The results of FTIR analysis of the OHF modified with VTAS have confirmed the reaction of silanization. This result was also confirmed by the test of water absorption behavior of the composites. The XRD spectra show the rate of crystallinity of UTOHF, which decreased from 45 to 34% for the treated OHF. This decrease was attributed to the increase in the amorphous part. The thermal behavior of UTOHF and OHFTS are almost similar, except for the onset temperature of decomposition for the UTOHF which is 210.9°C and for the OHFTS which is 201.3°C.

The mechanical behavior of PE/OHF composites shows that with the increase of UTOHF, the stress and elongation at break decreases, whereas the elastic modulus and shore hardness increases. We noticed that after chemical modification, the stress at break increases, particularly the composites treated by MAPE have a better tensile strength when compared with those treated by the VTAS. This can be explained by the capacity of MAPE to form strong interfacial adhesion between the PE and the OHF and consequently a better transfer of stress between the two phases. In contrast, the deformation at break increases with the use of polyethylene maleated, whereas it decreases with the use of vinyl silane. The opposite effect is observed for Young's modulus. With regard to the impact resistance, the resilience decreases with the increase of the flour and with the treatment.

The rate of water absorption depends on the immersion time, the rate of OHF, and also on the types of treatment, which gives a more or less hydrophobic character to the materials. The thermal analysis has shown that the incorporation of the UTOHF in the PE matrix decreases the temperature of beginning decomposition. The composites modified by the MAPE reveal a better thermal stability when compared with the composites modified by the VTAS and untreated composites. As a conclusion, the two chemical treatments contribute to the improvement of the interfacial properties of PE/OHF.

References

1. Roy, D.; Massey, S.; Adnot, A.; Rjeb, A. eXPRESS Polym Lett 2007, 1, 506.
2. Panayiotou, C.; Tserki, V.; Matzinos, P.; Kokkou, S. Compos A 2005, 36, 965.
3. Wolfgang, G.; Aleksandra, S.; Ulrich, M. Compos A 2006, 37, 1406.
4. Hyun-Joong, K.; Han-Seung, Y.; Michael, P.; Wolcott.; Hee-Soo, K.; Sumin, K. Compos Struct 2007, 79, 369.
5. Li, Q.; Matuana, L. J Appl Polym Sci 2003, 88, 278.
6. Corrales, F.; Vilasec, F.; Llop, M.; Gironès, J.; Méndez, J. A.; Mutj, P. J Hazard Mater 2007, 144, 730.
7. Bledzki, A. K.; Omar, F. Compos Sci Technol 2004, 64, 693.
8. Marais, S.; Bessadok, A.; Gouanve, F.; Colasse, L.; Zimmerlin, I.; Roudesli, S.; Métayer, M. Compos Sci Technol 2007, 67, 685.
9. Lu, J. Z.; Wu, Q.; McNabb, H. S. Wood Fiber Sci 2000, 32, 88–104.
10. Viksne, A.; Bledzki, A. K.; Letman, M.; Rence, L. Compos A 2005, 36, 789.
11. Aurrekoetxea, J.; Sarrionandia, M.; Gómez, X. Wear 2008 265, 606.
12. Garcia Martinez, J. M.; Laguna, O.; Collar, E. P. J Appl Polym Sci 1998, 68, 483.
13. Van Soest, P. J.; Wine, R. H. J—Assoc Off Anal Chem 1963, 46, 830.
14. Van Soest, P. J.; Wine, R. H. J—Assoc Off Anal Chem 1968, 51, 780.
15. Gassan, J.; Bledzki, A. K. Compos A 1997, 28, 1001.
16. Kaci, M.; Djidjelli, H.; Boukerrou, A.; Zaidi, L. eXPRESS Polym Lett 2007, 1, 467.
17. Bengtsson, M.; Oksman, K. Compos A 2006, 37, 752.
18. Nah, C.; Hong, C. K.; Hwang, I.; Kim, N.; Park, D. H.; Hwang, B. S. J Ind Eng Chem 2008, 14, 71.
19. Boufi, S.; Abdelmouleh, M.; Belgacem, M. N.; Dufresne, A. Compos Sci Technol 2007, 67, 1627.

20. Heritage, K. J.; Mann, J.; Roldan-Gonzales, L. J Polym Sci Part A: Polym Chem 1963, 1, 671.
21. Bhaduri, S. K.; Mathew, A.; Day, M. D.; Pandey, S. N. Cell Chem Technol 1994, 28, 391.
22. Kosik, M.; Luzakova, V.; Reiser, V. Cell Chem Technol 1972, 6, 589.
23. Ersan, P.; Basak Burcu, U.; Eren Putun, A. J Anal Appl Pyrolysis 2007, 79, 147.
24. Elesini, U. S.; Cuden, A. P.; Richards, A. F. Acta Chim Slov 2002, 49, 815.
25. Shiraishi, N.; Matsunaga, T.; Yokota, T.; Hayashi, Y. J Appl Polym Sci 1979, 24, 2347.
26. Marcovich, N. E.; Reboredo, M. M.; Aranguren, M. I. Thermochim Acta 2001, 372, 45.
27. Bing, L.; Yuhui, H.; Guangmin, C. J Appl Polym Sci 1997, 66, 1561.
28. Dufresne, A.; Pasquini, D.; Teixeira, E. M.; Curvelo, A. A. S.; Mohamed Naceur, B. Compos Sci Technol 2008, 68, 193.
29. Djidjelli, H.; Benachour, D.; Boukerrou, A.; Zefouni, O.; Martinez-Véga, J.; Farenc, J.; Kaci, M. eXPRESS Polym Lett 2007, 1, 846.
30. Sabu, T.; Maya Jacob, J.; Bejoy, F.; Varughese, K. T. Compos A 2008, 39, 352.
31. Dobircau, L.; Sreekumar, P. A.; Saiah, R.; Leblanc, N.; Terrié, C.; Gattin, R.; Saiter, J. M. Compos A 2009, 40, 329.
32. Demir, H.; Atikler, U.; Balkose, D.; Tıhmınlıoglu, F. Compos A 2006, 37, 447.
33. Nachtigall, S. M. B.; Cerveira, G. S.; Rosa, S. M. L. Polym Test 2007, 26, 619.
34. Pasquini, D.; Belgacem, M. N.; Gandini, A.; Curvelo, A. A. S. J Colloid Interface Sci 2006, 295, 79.